ELSEVIER   PII S0891-5849(99)00137-9

Original Contribution

EVIDENCE FOR FREE RADICAL FORMATION DURING THE OXIDATION OF 2′-7′-DICHLOROFLUORESCIN TO THE FLUORESCENT DYE 2′-7′-DICHLOROFLUORESCEIN BY HORSERADISH PEROXIDASE: POSSIBLE IMPLICATIONS FOR OXIDATIVE STRESS MEASUREMENTS

Cristina Rota, Colin F. Chignell, and Ronald P. Mason

Laboratory of Pharmacology and Chemistry, National Institute of Environmental Health Sciences, National Institutes of Health, Research Triangle Park, NC, USA

Abstract—The oxidation of 2′-7′-dichlorofluorescin (DCFH) to the fluorescent 2′-7′-dichlorofluorescein (DCF) by horseradish peroxidase (HRP) was investigated by fluorescence, absorption, and electron spin resonance spectroscopy (ESR). As has been previously reported, HRP/H_2O_2 oxidized DCFH to the highly fluorescent DCF. However, DCF fluorescence was still observed when H_2O_2 was omitted, although its intensity was reduced by 50%. Surprisingly, the fluorescence increase, in the absence of exogenous H_2O_2, was still strongly inhibited by catalase, demonstrating that H_2O_2 was present and necessary for DCF formation. H_2O_2 was apparently formed during either chemical or enzymatic deacetylation of 2′-7′-dichlorofluorescin diacetate (DCFH-DA), probably by auto-oxidation. Spectrophotometric measurements clearly showed that DCFH could be oxidized either by HRP-compound I or HRP-compound II with the obligate generation of the DCF semiquinone free radical (DCF$^{\bullet-}$). Oxidation of DCF$^{\bullet-}$ to DCF by oxygen would yield superoxide ($O_2^{\bullet-}$). ESR spectroscopy in conjunction with the spin trap 5,5-dimethyl-1-pyrroline *N*-oxide (DMPO) revealed the presence of both superoxide and hydroxyl radicals in the DCFH/H_2O_2/HRP system. Both radicals were also detected in the absence of added H_2O_2, although the intensities of the resultant adducts were decreased. This work demonstrates that DCF fluorescence cannot be used reliably to measure $O_2^{\bullet-}$ in cells because $O_2^{\bullet-}$ itself is formed during the conversion of DCFH to DCF by peroxidases. The disproportionation of superoxide forms H_2O_2 which, in the presence of peroxidase activity, will oxidize more DCFH to DCF with self-amplification of the fluorescence. Because the deacetylation of DCFH-DA, even by esterases, can produce H_2O_2, the use of this probe to measure H_2O_2 production in cells is problematic.   © 1999 Elsevier Science Inc.

Keywords—2′-7′-Dichlorofluorescin, 2′-7′-Dichlorofluorescein, Oxidation, Free radical, Superoxide, Hydrogen peroxide, Spin trapping

INTRODUCTION

Fluorogenic probes have been widely employed to monitor oxidative activity in cells [1]. Fluorometric assays are based on the use of the chemically reduced, nonfluorescent forms of highly fluorescent dyes such as fluorescein and rhodamine that are oxidized to the parent dye molecule, resulting in a dramatic increase in fluorescence intensity.

2′-7′-Dichlorofluorescin (DCFH) is widely used to measure oxidative stress in cells. When the diacetate form of DCFH is added to cells, it diffuses across the cell membrane and is hydrolyzed by intracellular esterases to liberate DCFH which, upon reaction with oxidizing species, forms its 2-electron oxidation product, the highly fluorescent compound 2′-7′-dichlorofluorescein (DCF). The fluorescence intensity can be easily measured and is the basis of the popular cellular assay for oxidative stress. The oxidation of DCFH is thought to occur as a result of the reaction of H_2O_2 with peroxidase, cytochrome *c*, or Fe^{2+} [2–5]. Peroxynitrite, but not H_2O_2 or superoxide free radical, can oxidize DCFH directly [5,6].

Although this assay is extensively used, there are still controversies regarding its validity. It remains unclear

Address correspondence to: Ronald P. Mason, NIH/NIEHS, MD F0-01, P.O. Box 12233, Research Triangle Park, North Carolina, 27709, USA; Tel: (919) 541-3910; Fax: (919) 541-1043; E-Mail: mason4@niehs.nih.gov.
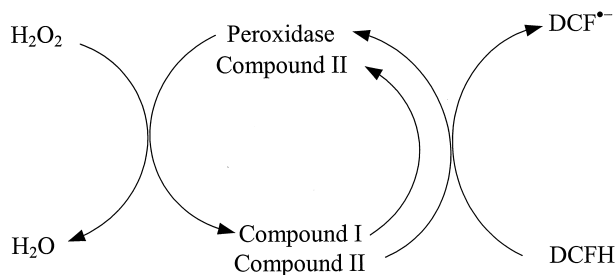
Scheme 1. The peroxidase oxidation of DCFH

which oxidative species is responsible for the oxidation of DCFH. DCFH oxidation can result from several reactive intermediates, causing difficulties in the interpretation of the data. Moreover, there is some controversy in the literature concerning the effect of the addition of superoxide dismutase (SOD) on oxidative stress in cells as monitored using the DCFH test. Some studies report an inhibitory effect by superoxide dismutase [7–20] whereas almost the same number of studies report no effect [21–31]. Lebel et al. pointed out the necessity of using caution in the interpretation of specific reactive oxygen species involved in the oxidation of DCFH to DCF in biologic systems and that HRP could oxidize DCFH directly [2]. In a previous study, we demonstrated that the photoreduction of DCF (the oxidized, fluorescent form of DCFH) results in the formation of the DCF semiquinone free radical (DCF$^{\bullet-}$) which, under aerobic conditions, is oxidized by oxygen to the parent dye, concomitantly forming superoxide radical [32].

In the present work, the reaction of DCFH with horseradish peroxidase in the presence or absence of added H$_2$O$_2$ was investigated to understand better the chemistry of the DCF assay. We employed the electron spin resonance spectroscopy spin trapping technique to evaluate free radical formation and measured the fluorescence developed during the reactions. We also followed the formation of HRP-compound I and HRP-compound II.

Our results indicate that when DCFH reacts with HRP-compound I or HRP-compound II, DCFH is oxidized to the semiquinone free radical DCF$^{\bullet-}$, reducing the horseradish peroxidase enzyme intermediate (Scheme 1). Then DCF$^{\bullet-}$ is air-oxidized to DCF with the concomitant generation of superoxide radicals.

MATERIALS AND METHODS

Materials

Horseradish peroxidase type VI-A (HRP), porcine liver esterase, and diethylenetriamine pentaacetic acid (DTPA) were purchased from Sigma Chemicals Co. (St. Louis, MO, USA). The spin trap 5,5-dimethyl-1-pyrroline *N*-oxide (DMPO) was also purchased from Sigma, purified by vacuum distillation at ambient temperature, and stored at $-70°C$ until use. Dimethyl sulfoxide (DMSO) was purchased from Aldrich (Milwaukee, WI, USA). Concentrations of horseradish peroxidase were determined by using the extinction coefficient $\varepsilon = 102$ mM^{-1}cm^{-1} at 403 nm [33]. Tris (tris-hydroxymethyl-aminomethane) and Chelex 100 were purchased from Bio-Rad Laboratories (Hercules, CA, USA). 2′-7′-Di-
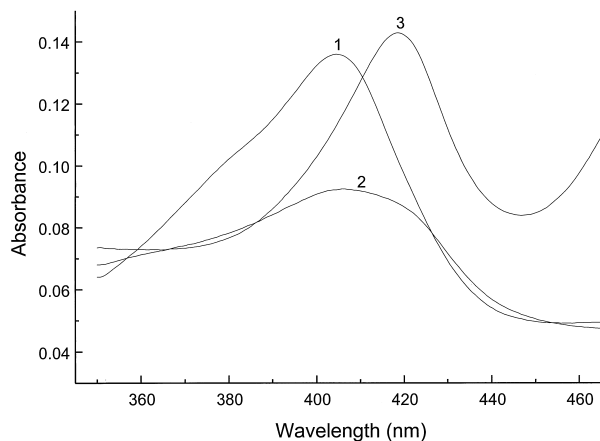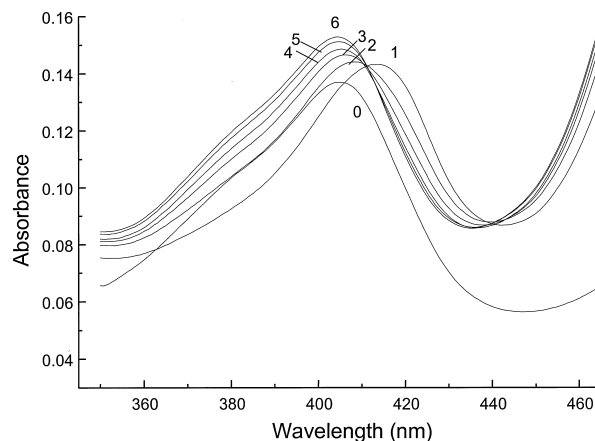

Fig. 1. Absorption spectra of horseradish peroxidase, HRP-compound I, and HRP-compound II. HRP was diluted to a final concentration of 1 μM in Tris-HCl buffer and scanned 2 min after mixing (scan 1). Scan 2 was taken immediately after the addition of 16 μM H$_2$O$_2$; scan 3 was taken immediately after the subsequent addition of 2.5 μM DCFH. All spectra were recorded at a rate of 5 nm/s, yielding a complete spectrum in 50 s. Absorption from 0.04 to 0.15 was presented to better show the spectral changes.

Fig. 2. Spectral changes during the reaction of DCFH with H$_2$O$_2$ and horseradish peroxidase. HRP was diluted to a final concentration of 1 μM in Tris-HCl buffer and incubated for 2 min at room temperature. Scan 0 was taken 1 min after the addition of 5 μM DCFH. Scans 1–6 were recorded immediately after the addition of 1.6 μM H$_2$O$_2$. All spectra were recorded at a rate of 5 nm/s, yielding a complete spectrum every 100 s. Absorption from 0.04 to 0.16 was presented to better show the spectral changes.
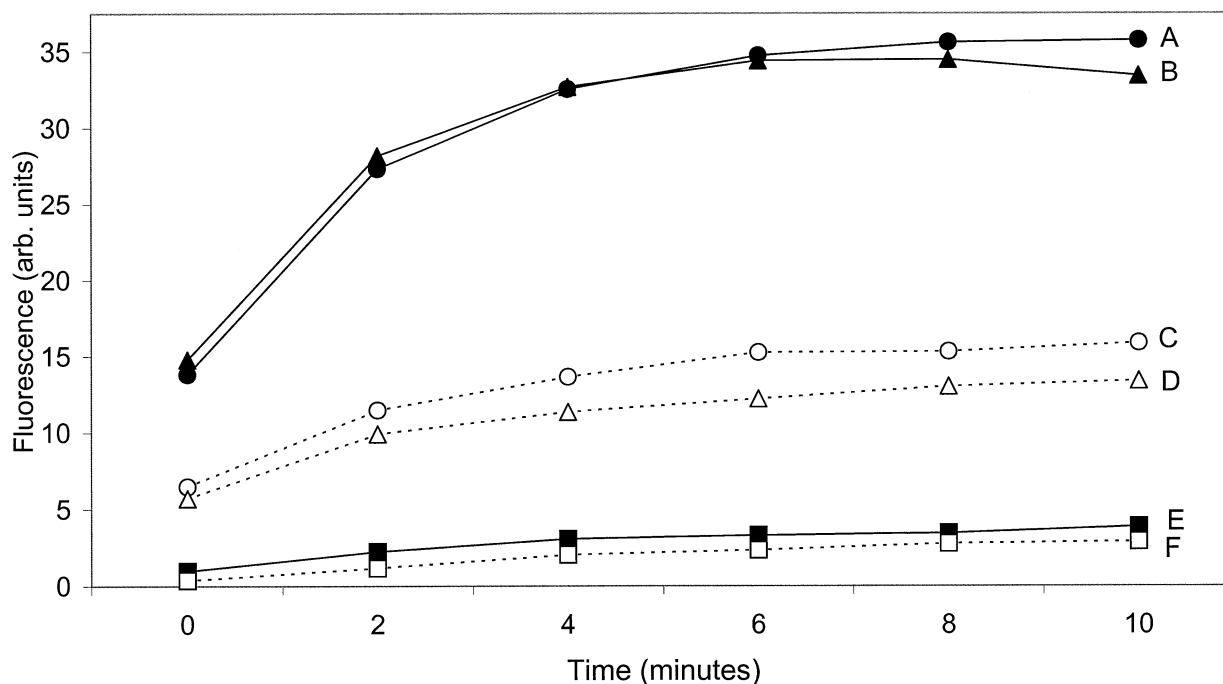
Fig. 3. Fluorescence intensity at 522 nm generated during reaction of DCFH with HRP in the presence or absence of added H_2O_2. Trace A represents the fluorescence generated by a reaction mixture containing 10 μM DCFH, 32 μM H_2O_2 and 0.2 μM HRP. Trace B, same as A, but with the addition of 50 μg/ml SOD. Trace C, the fluorescence generated by a reaction mixture containing 10 μM DCFH and 0.2 μM HRP. Trace D, same as trace C, but with the addition of SOD (50 μg/ml). Trace E, same as trace A, but with the addition of 150 μg/ml catalase. Trace F, same as trace C, but with the addition of 150 μg/ml catalase. The instrument settings are reported under Materials and Methods. arb. units = arbitrary units.

chlorofluorescin diacetate (also known as 2′-7′-dichlorodihydrofluorescein diacetate, DCFH-DA) was purchased from Molecular Probes (Eugene, OR, USA). DCFH was prepared following the method of Cathcart et al. [34]; DCFH-DA in methanol was chemically hydrolyzed at basic pH. This deesterification proceeded in the dark at room temperature for 30 min; then the mixture was neutralized with Tris-HCl buffer, pH 7.4. In the experiments shown in Figs. 1 and 2, the deesterification solution was added directly to the cuvette to avoid excessive dilution of the sample. For enzymatic de-esterification 500 μM DCFH-DA in a methanol-buffer solution reacted with esterase (100 units) in the dark at room temperature for 1 h at neutral pH. Catalase (from beef liver, 65,000 U/mg) and superoxide dismutase (SOD) (from bovine erythrocytes, 5000 U/ml) were purchased from Boehringer-Mannhein (Indianapolis, IN, USA). Hydrogen peroxide (30%) was purchased from Fisher Scientific (Pittsburgh, PA, USA). Stock concentrations of H_2O_2 in deionized water were determined by using the extinction coefficient $\varepsilon = 43.6$ $M^{-1}cm^{-1}$ at 240 nm [35]. High-performance liquid chromatography (HPLC)-grade water was purchased from JT Baker (Phillipsburg, NJ, USA).

All the reactions werecarried out in 50 mM Tris buffer adjusted to pH 7.4 with hydrochloric acid. The Tris-HCl buffer was treated with Chelex 100 resin to remove traces of transition metal ions and contained 50 μM DTPA to minimize the possibility of trace-metal catalysis.

DCFH was stored protected from the light. Sample preparation and experiments were performed in the dark. All reactions were initiated with the addition of HRP. In the samples where DCFH was omitted, an equal volume of methanol/0.01 N NaOH/Tris buffer (1:4:20 v/v/v) was added.

Electron spin resonance experiments

ESR spectra were recorded using a Bruker ECS-106 spectrometer (Billerica, MA, USA) operating at 9.77 GHz with a modulation frequency of 50 kHz and a TM_{110} cavity. Spectra were recorded on an IBM-compatible computer interfaced to the spectrometer. The computer simulations were performed using a program that is available through the Internet (http://epr.niehs.nih.gov/). The details of the program were described in a recent publication [36].

Fluorescence spectroscopy

Fluorometric measurements were made with an Aminco-Bowman spectrophotofluorometer (American Instrument Co., Silver Spring, MD, USA) . Fluorescence levels were measured every 2 min for a total of 10 min; the excitation light was excluded between measurements. Slit settings were 1.2 nm for excitation and 36 nm for emission. DCF-fluorescence was excited at 498 nm and the emission was measured at 522 nm in a quartz cuvette with a 10-mm light-path.

Horseradish peroxidase, HRP-compound I,
HRP-compound II, visible spectra

All spectral measurements were carried out with an SLM Aminco DW-2000 UV-Vis spectrophotometer (Urbana, IL, USA) equipped with a dual beam. The samples were read against a blank containing Tris buffer. In the experiments (Fig. 2), the reference contained Tris-HCl buffer, methanol, and 0.01 N NaOH in the same proportions present in the samples.

RESULTS

The visible spectra of resting horseradish peroxidase, HRP-compound I and HRP-compound II are shown in Fig. 1. Scan 1 shows the spectrum of a solution of 1 μM HRP; compound I was generated after the addition of 16 μM H_2O_2 (scan 2). The addition of 2.5 μM DCFH induced the formation of compound II (scan 3). The higher value of the maximum absorption for compound II is due to its higher extinction coefficient ($\varepsilon = 105$ mM^{-1}cm^{-1} at 420 nm) versus that of compound I ($\varepsilon = 102$ mM^{-1}cm^{-1} at 403 nm) [33]. The reaction between horseradish peroxidase and H_2O_2 generates HRP-compound I; then DCFH reduces HRP-compound I to HRP-compound II, with the formation of the DCF$^{\bullet-}$ semiquinone free radical. The absorption spectra are little altered by the addition of DCFH and its consequent oxidation to DCF. DCF is characterized by an absorption maximum at 502 nm. The DCF absorption peak starts around 425 nm, becoming really evident only above 440 nm.

The spectral transformations during the turnover of horseradish peroxidase in the presence of H_2O_2 and DCFH are shown in Fig. 2. HRP was incubated with DCFH (scan 0); then H_2O_2 was added to the system (scans 1–6). The consequent formation of compound II is demonstrated by the appearance of an isobestic point for resting HRP and compound II at 412 nm [37]. Scans 2–6 show the disappearance of compound II and reformation of native HRP. The small shifting of the absorption peak of compound II and the higher value of the HRP maximum absorption in scans 2–6 are probably due to the presence, in that region, of the shoulder of the absorption peak of the DCF formed during the experiment.

The oxidation of the nonfluorescent DCFH to the fluorescent dye DCF, measured as increased fluorescence at 522 nm, is shown in Fig. 3. The reaction mixture consisted of 10 μM DCFH, 32 μM H_2O_2 and 0.2 μM HRP. The excitation light ($\lambda = 498$ nm) was excluded between measurements, and the emission light ($\lambda = 522$ nm) recorded every 2 min for a total of 10 min. The level of fluorescence increased, reaching a maximum at 8 min (Fig. 3, trace A). The addition of SOD did not have any effect (Fig. 3, trace B), but the addition of catalase to the system almost completely prevented the oxidation of DCFH (Fig. 3, trace E). The omission of HRP completely prevented the development of fluorescence (data not shown). When H_2O_2 was substituted with HPLC-grade water, the level of fluorescence decreased more than 50%, but was still easily detectable although variable (Fig. 3, trace C). SOD showed a weak inhibitory effect (Fig. 3, trace D). Even in the absence of added H_2O_2, catalase almost completely inhibited fluorescence development (Fig. 3, trace F). To work under more physiologic conditions, the experiment was repeated, deacetylating DCFH-DA by esterase at neutral pH (Fig. 4). As shown in Fig. 4, fluorescence development was very similar to that shown in Fig. 3. In this case, the fluorescence development in the absence of added H_2O_2 was often stronger, but still variable and was still completely inhibited by catalase. This demonstrates that some H_2O_2 had been formed during either chemical or enzymatic deacetylation of DCFH-DA, probably from DCFH auto-oxidation. This result is inconsistent with DCFH serving directly as a reducing substrate for HRP as proposed [2]. The addition of 1.4 M DMSO, a well-known hydroxyl radical scavenger, to the system, did not have any effect on fluorescence (data not shown), demonstrating that hydroxyl radical does not contribute significantly to the peroxidase-catalyzed oxidation of DCFH. In addition, under our conditions neither catalase nor superoxide dismutase (with or without hydrogen peroxide) oxidized DCFH to DCF.

When the recording time was fixed and the H_2O_2 concentration was varied (to evaluate the dose-response relationship between H_2O_2 and fluorescence), the level of fluorescence increased monotonically with the H_2O_2 concentration, but the fluorescence intensity increment became smaller for H_2O_2 concentrations higher than 1μM, with a plateau reached at around 10 μM (data not shown).

The ESR spin trapping technique was employed to investigate free radical formation during the turnover of horseradish peroxidase with H_2O_2 and DCFH. When 10 μM DCFH was incubated with 32 μM H_2O_2 and 0.2 μM HRP in the presence of the spin trap DMPO (200 mM), a mixture of two radical adducts was detected (Fig. 5). The
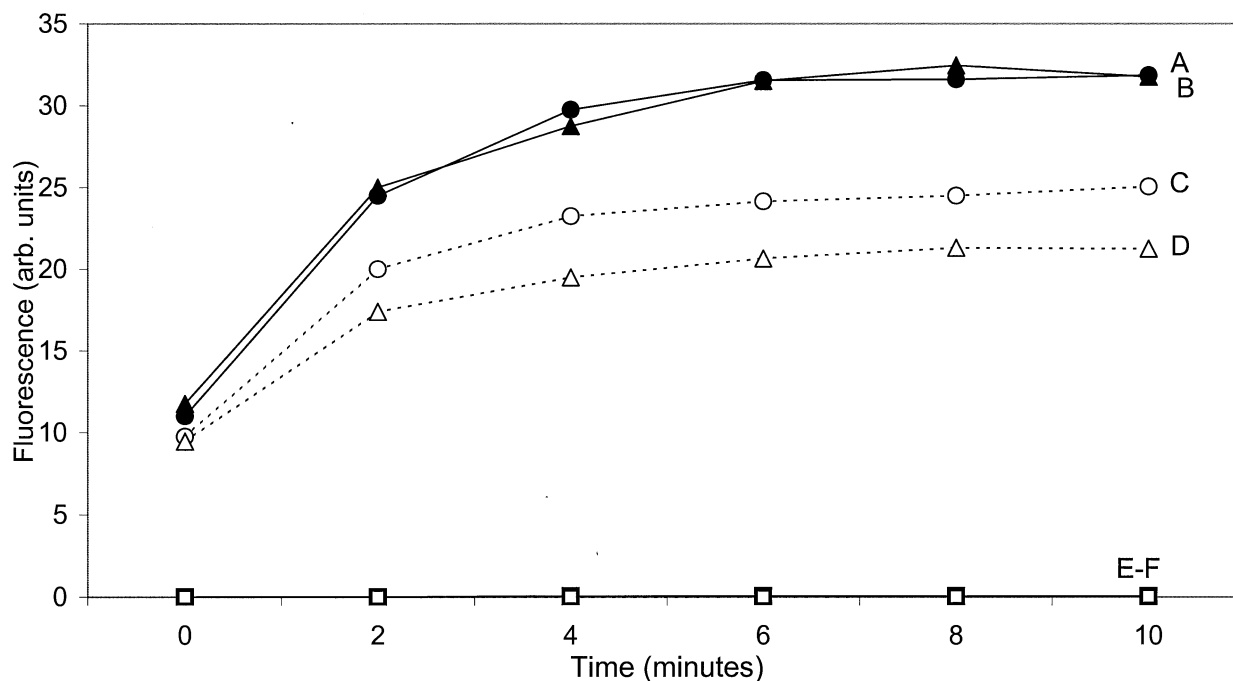
Fig. 4. Fluorescence intensity during reaction of DCFH (enzymatically deacetylated) with horseradish peroxidase in the presence or absence of added H_2O_2. Trace A represents the fluorescence generated by a reaction mixture containing 10 μM DCFH, 32 μM H_2O_2 and 0.2 μM HRP. Trace B, same as trace A, but with the addition of 50 μg/ml SOD. Trace C, the fluorescence generated by a reaction mixture containing 10 μM DCFH and 0.2 μM HRP. Trace D, same as trace C, but with the addition of SOD (50 μg/ml). Trace E, same as trace A, but with the addition of 150 μg/ml catalase. Trace F, same as trace C, but with the addition of 150 μg/ml catalase. The instrument settings are reported under Materials and Methods. arb. units = arbitrary units.

computer simulation employed to obtain the hyperfine coupling constants was superimposed on the experimental spectrum as a dashed line (Fig. 5, spectrum A). On the basis of the hyperfine coupling constants, the radical adducts were assigned as follows: DMPO/˙OH (a^N = 15.00 ± 0.08 G and a_β^H = 14.70 ± 0.05 G), which accounts for 35% of the radical concentration, and DMPO/˙OOH (a^N = 14.22 ± 0.08 G, a_β^H = 11.16 ± 0.05 G, and a_Y^H = 1.27 ± 0.01 G), which accounts for 65% of the radical concentration. The hyperfine coupling constants, obtained by averaging the values resulting from five experiments, were consistent with previously reported values for these adducts [38,39]. When DCFH or HRP was omitted, only a very weak signal was detected (Fig. 6, spectra B and D). The same signal was obtained from DMPO alone (Fig. 6, spectrum I). The addition of SOD or catalase completely inhibited the ESR signal (Fig. 6, spectra E and F), demonstrating the involvement of superoxide and hydrogen peroxide in the formation of these radical adducts. When oxygen was excluded, a very weak signal was also detected (Fig. 6, spectrum G). To obtain lower oxygen concentrations, buffer was bubbled with nitrogen directly in the ESR flat cell, and each reactant was added one at a time while still bubbling. When H_2O_2 was substituted with an equal volume of HPLC-grade water, a weak signal was obtained (Fig. 6, spectrum C) that had the typical characteristics of a DMPO/˙OH adduct and

was inhibited by SOD (Fig. 6, spectrum H). Typically, SOD totally inhibits DMPO/˙OOH formation or the formation of any radical adducts dependent on superoxide formation such as, in this case, DMPO/˙OH, because the reaction rate of superoxide with DMPO is extremely slow relative to that with SOD.

Using a higher concentration of horseradish peroxidase and more sensitive ESR conditions, we tried to identify the signal obtained in the system where H_2O_2 was omitted. A reaction mixture containing 10 μM DCFH and 1 μM HRP in the presence of 200 mM DMPO gave a mixture of two radical adducts (Fig. 7). The computer simulation employed to obtain the hyperfine coupling constants was superimposed on the experimental spectrum as a dashed line (Fig. 7, spectrum A). On the basis of the hyperfine coupling constants, the radical adducts were assigned as follows: DMPO/˙OH (a^N = 15.01 ± 0.02 G and a_β^H = 14.60 ± 0.02 G), which accounts for 64% of the radical concentration, and DMPO/˙OOH (a^N = 14.36 ± 0.03 G, a_β^H = 11.16 ± 0.05 G, and a_Y^H = 1.28 ± 0.01 G), which accounts for 36% of the radical concentration. As with the hydrogen peroxide-containing system, the hyperfine coupling constants, obtained by averaging the values resulting from four experiments, were consistent with previously reported values for these radical adducts [38,39]. When
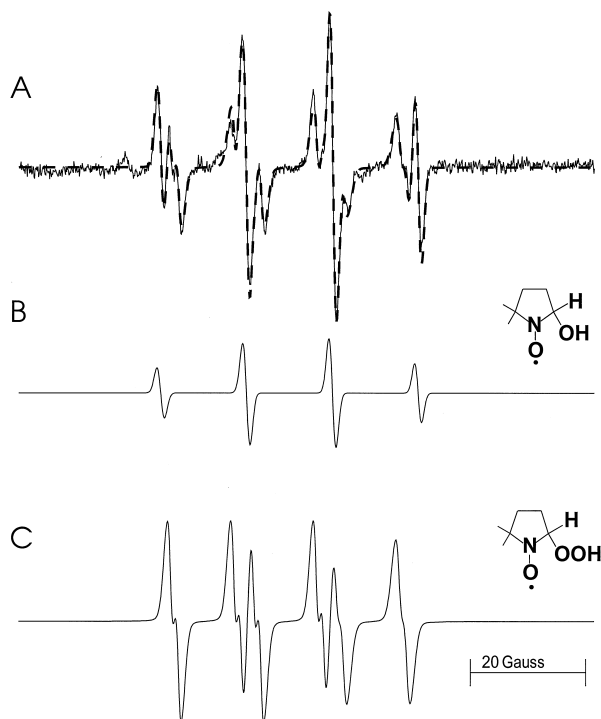
Fig. 5. Computer simulation and deconvolution of the ESR spectrum obtained from the reaction mixture containing DCFH, H_2O_2 DMPO, and horseradish peroxidase. Spectrum A is the computer simulation (dashed line) superimposed on the experimental spectrum obtained using 10 μM DCFH, 32 μM H_2O_2, 200 mM DMPO, and 0.2 μM HRP. Spectra B–C are the individual simulations of each species in the composite spectrum. The hyperfine coupling constants of each species are provided under Results. Spectrum B is the simulated spectrum for DMPO/˙OH. Spectrum C is the simulated spectrum for DMPO/˙OOH. Spectrometer conditions were modulation amplitude, 1 G; microwave power, 20 milliwatts; time constant, 0.328 s; conversion time, 0.655 s; scan time, 671 s; scan range, 100 G; and receiver gain, 4×10^5.
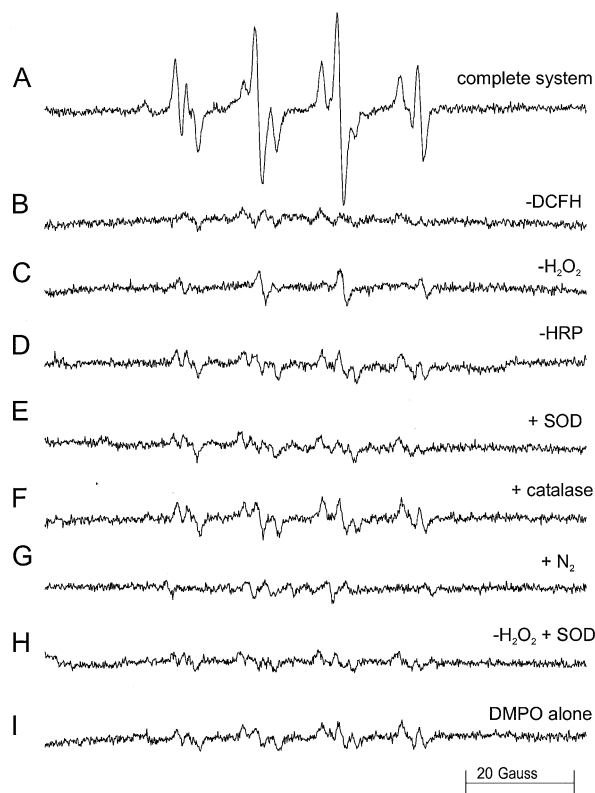

Fig. 6. ESR spectra of DMPO radical adducts produced by the reaction of DCFH with horseradish peroxidase in the presence of H_2O_2. Spectrum A is the ESR spectrum obtained from a reaction mixture containing 10 μM DCFH, 32 μM H_2O_2, 200 mM DMPO, and 0.2 μM HRP (the same spectrum as Fig. 5, spectrum A). Spectrum B is the same as spectrum A, except DCFH was omitted. Spectrum C was obtained using the conditions of spectrum A, except H_2O_2 was substituted with an equal volume of HPLC-grade water. Spectrum D is the same as spectrum A, but with omission of HRP. Spectrum E is the same as spectrum A, but with the addition of 50 μg/ml SOD. Spectrum F is the same as spectrum A, but with the addition of 150 μg/ml catalase. Spectrum G is the spectrum obtained using the conditions of spectrum A, but under anaerobic conditions. Spectrum H is the same as spectrum C, but with the addition of 50 μg/ml SOD. Spectrum I is the spectrum obtained using buffer and DMPO alone. Spectrometer conditions were as described in Fig. 5.

DCFH was absent, no signal was detected (Fig. 8, spectrum B). When HRP was omitted, the same signal obtained from DMPO alone was detected (Fig. 8, spectrum C). The fact that, in the absence of HRP, the background signal from the DMPO impurities was stronger than in the absence of DCFH (Fig. 6 spectra B, D and Fig. 8, spectra B, C) is probably due to HRP-catalyzed oxidation of nitroxide impurities to ESR-silent products. The addition of SOD completely inhibited the ESR signal (Fig. 8, spectrum D), demonstrating the involvement of superoxide. The addition of catalase had either a partial inhibitory effect or no effect at all (data not shown). Results similar to those shown in Figs. 5–8 were obtained when DCFH-DA hydrolysis was achieved enzymatically (data not shown).

The addition of DMSO (1.4 M) to both systems, with or without H_2O_2, resulted in the conversion of DMPO/ ˙OH to a carbon-centered radical adduct, presumably DMPO/˙CH_3 (data not shown), resulting from the ˙OH scavenger activity of DMSO [39]. This result demon- strates that DMPO/˙OH does not come from DMPO/ ˙OOH reduction to DMPO/˙OH by the peroxidase activity of horseradish peroxidase, but from hydroxyl radical trapping. DMPO/˙OH is much more stable than DMPO/ ˙OOH with a much longer lifetime; therefore, under steady state conditions, spin trapping experiments will over-represent the DMPO/ ˙OH rate of formation relative to that of DMPO/ ˙OOH.

DISCUSSION

This investigation extends previous studies showing that when DCFH reacts with horseradish peroxidase in the presence or absence of added H_2O_2, the molecule is
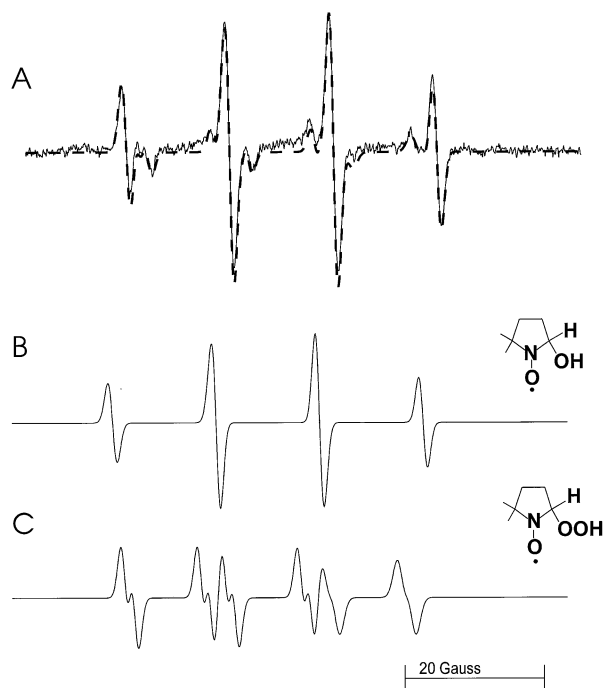
Fig. 7. Computer simulation and deconvolution of the ESR spectrum obtained from the reaction mixture containing DCFH, H_2O, DMPO, and horseradish peroxidase. Spectrum A is the computer simulation (dashed line) superimposed on the experimental spectrum obtained using 10 μM DCFH, 200 mM DMPO, and 1 μM HRP. Spectra B–C are the individual simulations of each species in the composite spectrum. The hyperfine coupling constants of each species are provided under Results. Spectrum B is the simulated spectrum for DMPO/•OH. Spectrum C is the simulated spectrum for DMPO/•OOH. Spectrometer conditions were modulation amplitude, 1 G; microwave power, 40 milliwatts; time constant, 1.31 s; conversion time, 1.31 s; scan time, 1342 s; scan range, 80 G; and receiver gain, 4×10^5.

Fig. 8. ESR spectra of DMPO radical adducts produced by the reaction of horseradish peroxidase with DCFH in the presence of H_2O. Spectrum A is the ESR spectrum obtained from a reaction mixture containing 10 μM DCFH, 200 mM DMPO, and 1 μM HRP (the same spectrum as Fig. 7, spectrum A). Spectrum B is the same as spectrum A, except DCFH was omitted. Spectrum C is the same as spectrum A, except HRP was omitted. Spectrum D is the same as spectrum A, but with the addition of 50 μg/ml SOD. Spectrum E is the spectrum obtained using buffer and DMPO alone.

oxidized, producing the fluorescent dye DCF. Visible spectrophotometry confirms the expected formation of HRP-compound I and compound II. Unexpectedly, ESR spin trapping investigations demonstrate the formation of hydroxyl and superoxide radical adducts. Another unexpected finding from the fluorescence measurements is the inhibiting effect of catalase in all the experiments, even when no H_2O_2 is added, providing evidence for hydrogen peroxide formation in all systems.

Horseradish peroxidase, upon reacting with H_2O_2, is converted to HRP-compound I. HRP-compound I (or compound II, resulting from the reaction of compound I with DCFH) oxidizes DCFH to $DCF^{\bullet -}$ semiquinone free radical (Scheme 1). $DCF^{\bullet -}$ is oxidized to the fluorescent compound DCF by oxygen, with the production of superoxide radical. The entire mechanism is presented in Scheme 2.

Dismutation of superoxide, spontaneously or by SOD, will generate hydrogen peroxide, causing amplification of the peroxidase-catalyzed reaction. Finally, the finding that SOD partially inhibits fluorescence formation in the
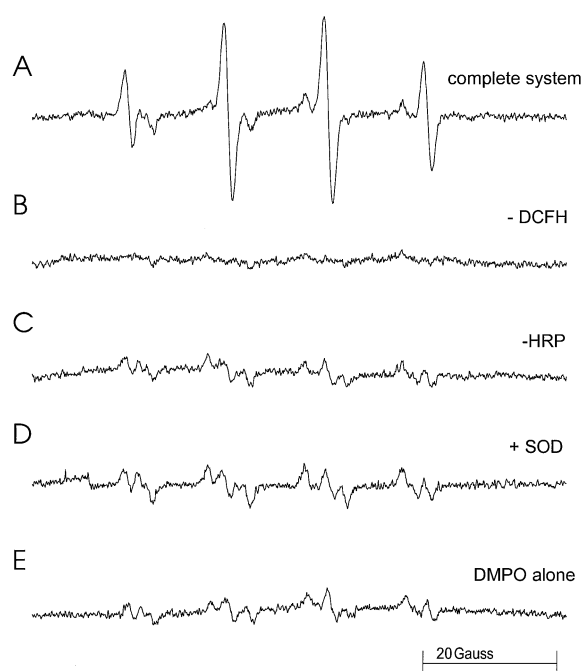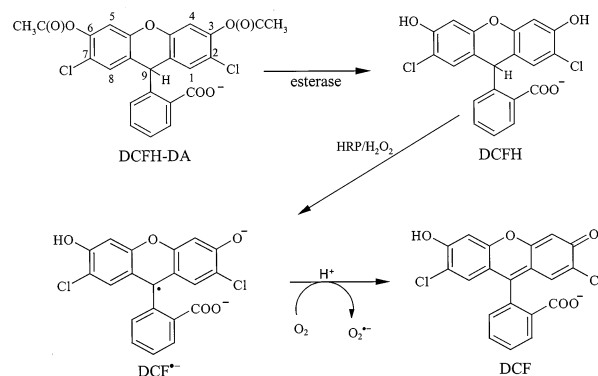
absence of added H_2O_2 (Figs. 3 and 4) could provide an explanation for the controversy existing in literature regarding the superoxide dismutase effect on the DCFH test for oxidative stress.

The formation of superoxide (and hydrogen peroxide) via this mechanism is probably true also for other flu-

Scheme 2. The proposed mechanism for the HRP-catalyzed DCFH oxidation to DCF

orometric probes with molecular characteristics similar to DCFH, in particular dihydrorhodamine 123, widely used as an indicator for respiratory burst activity [40], hydrogen peroxide [5] peroxynitrite [41,42], and reactive oxygen species [43,44] production in cells.

This study implies that DCFH cannot be used to measure superoxide formation in cells because the oxidation of this compound leads to the formation of superoxide. In addition, oxidation of DCFH leads to H_2O_2 production via the disproportionation of this superoxide. Moreover, enzymatic deacetylation of DCFH-DA must result in trace H_2O_2 production, because the HRP-dependent oxidation of DCFH is totally inhibited by catalase even in the absence of added hydrogen peroxide. Presumably, deacetylated DCFH auto-oxidizes to form trace amounts of hydrogen peroxide, implying that the use of this probe to measure H_2O_2 production in cells is problematic. Several issues with regard to DCFH oxidation in the measurement of intracellular hydrogen peroxide formation must be considered in future work. First, the oxidation of DCFH to DCF will form superoxide which, upon disproportionation, generates hydrogen peroxide, so the assay is inherently autocatalytic. Second, because DCFH auto-oxidation appears to form trace amounts of hydrogen peroxide, detection of hydrogen peroxide with this assay appears to be predestined. Third, although changes in the rate of DCF formation may result from corresponding changes in the rate of hydrogen peroxide formation, potential changes in peroxidase activity are, at least, of equal importance. Fourth, the oxidation of DCFH by HRP should be more or less representative of its oxidation by many mammalian peroxidases and hemoproteins with peroxidase activity such as methemoglobin. In fact, the peroxidase activity of prostaglandin H synthase is known to oxidize DCFH to DCF [45].

REFERENCES

[1] Tsuchiya, M.; Suematsu, M.; Suzuki, H. *In vivo* visualization of oxygen radical-dependent photoemission. *Methods Enzymol.* **233:** 128–140; 1994.

[2] LeBel, C. P.; Ischiropoulos, H.; Bondy, S. C. Evaluation of the probe 2′,7′-dichlorofluorescin as an indicator of reactive oxygen species formation and oxidative stress. *Chem. Res. Toxicol.* **5:**227–231; 1992.

[3] Rothe, G.; Valet, G. Flow cytometric analysis of respiratory burst activity in phagocytes with hydroethidine and 2′,7′-dichlorofluorescin. *J. Leukoc. Biol.* **47:**440–448; 1990.

[4] Huang, X.; Frenkel, K.; Klein, C. B.; Costa, M. Nickel induces increased oxidants in intact cultured mammalian cells as detected by dichlorofluorescein fluorescence. *Toxicol. Appl. Pharmacol.* **120:**29–36; 1993.

[5] Royall, J. A.; Ischiropoulos, H. Evaluation of 2′,7′-dichlorofluorescin and dihydrorhodamine 123 as fluorescent probes for intracellular H_2O_2 in cultured endothelial cells. *Arch. Biochem. Biophys.* **302:**348–355; 1993.

[6] Kooy, N. W.; Royall, J. A.; Ischiropoulos, H. Oxidation of 2′,7′-dichlorofluorescin by peroxynitrite. *Free Radic. Res.* **27:**245–254; 1997.

[7] Atlante, A.; Gagliardi, S.; Minervini, G. M.; Ciotti, M. T.; Marra, E.; Calissano, P. Glutamate neurotoxicity in rat cerebellar granule cells: a major role for xanthine oxidase in oxygen radical formation. *J. Neurochem.* **68:**2038–2045; 1997.

[8] Burow, S.; Valet, G. Flow-cytometric characterization of stimulation, free radical formation, peroxidase activity and phagocytosis of human granulocytes with 2,7-dichlorofluorescein (DCF). *Eur. J. Cell Biol.* **43:**128–133; 1987.

[9] Fukumura, D.; Kurose, I.; Miura, S.; Tsuchiya, M.; Ishii, H. Oxidative stress in gastric mucosal injury: role of platelet-activating factor-activated granulocytes. *J. Gastroenterol.* **30:**565–571; 1995.

[10] Gunasekar, P. G.; Kanthasamy, A. G.; Borowitz, J. L.; Isom, G. E. NMDA receptor activation produces concurrent generation of nitric oxide and reactive oxygen species: implication for cell death. *J. Neurochem.* **65:**2016–2021; 1995.

[11] Gunasekar, P. G.; Sun, P. W.; Kanthasamy, A. G.; Borowitz, J. L.; Isom, G. E. Cyanide-induced neurotoxicity involves nitric oxide and reactive oxygen species generation after N-methyl-D-aspartate receptor activation. *J. Pharmacol. Exp. Ther.* **277:**150–155; 1996.

[12] Hagar, H.; Ueda, N.; Shah, S. V. Role of reactive oxygen metabolites in DNA damage and cell death in chemical hypoxic injury to LLC-PK$_1$ cells. *Am. J. Physiol.* **271:**F209–215; 1996.

[13] Horio, F.; Fukuda, M.; Katoh, H.; Petruzzelli, M.; Yano, N.; Rittershaus, C.; Bonner-Weir, S.; Hattori, M. Reactive oxygen intermediates in autoimmune islet cell destruction of the NOD mouse induced by peritoneal exudate cells (rich in macrophages) but not T cells. *Diabetologia* **37:**22–31; 1994.

[14] Kurose, I.; Saito, H.; Suematsu, M.; Fukumura, D.; Miura, S.; Morizane, T.; Tsuchiya, M. Kupffer cell-mediated oxidative stress on colon cancer cell line visualized by digital imaging fluorescence microscopy. *Cancer Lett.* **59:**201–209; 1991.

[15] Kurose, I.; Miura, S.; Fukumura, D.; Yonei, Y.; Saito, H.; Tada, S.; Suematsu, M.; Tsuchiya, M. Nitric oxide mediates Kupffer cell-induced reduction of mitochondrial energization in hepatoma cells: a comparison with oxidative burst. *Cancer Res.* **53:**2676–2682; 1993.

[16] Oyama, Y.; Hayashi, A.; Ueha, T.; Maekawa, K. Characterization of 2′,7′-dichlorofluorescin fluorescence in dissociated mammalian brain neurons: estimation on intracellular content of hydrogen peroxide. *Brain Res.* **635:**113–117; 1994.

[17] Puntarulo, S.; Cederbaum, A. I. Role of cytochrome *P*-450 in the stimulation of microsomal production of reactive oxygen species by ferritin. *Biochim. Biophys. Acta* **1289:**238–246; 1996.

[18] Reid, M. B.; Haack, K. E.; Franchek, K. M.; Valberg, P. A.; Kobzik, L.; West, M. S. Reactive oxygen in skeletal muscle. I. Intracellular oxidant kinetics and fatigue in vitro. *J. Appl. Physiol.* **73:**1797–1804; 1992.

[19] Saito, H.; Fukumura, D.; Kurose, I.; Suematsu, M.; Tada, S.; Kagawa, T.; Miura, S.; Morizane, T.; Tsuchiya, M. Visualization of oxidative processes at the cellular level during neutrophil-mediated cytotoxicity against a human hepatoma cell line, HCC-M. *Int. J. Cancer* **51:**124–129; 1992.

[20] Scott, J. A.; Homcy, C. J.; Khaw, B. A.; Rabito, C. A. Quantitation of intracellular oxidation in a renal epithelial cell line. *Free Radic. Biol. Med.* **4:**79–83; 1988.

[21] Yang, C.-F.; Shen, H.-M.; Shen, Y.; Zhuang, Z.-X.; Ong, C.-N. Cadmium-induced oxidative cellular damage in human fetal lung fibroblasts (MRC-5 cells). *Environ. Health Perspect.* **105:**712–716; 1997.

[22] Zhu, H.; Bannenberg, G. L.; Moldéus, P.; Shertzer, H. G. Oxidation pathways for the intracellular probe 2′,7′- dichlorofluorescin. *Arch. Toxicol.* **68:**582–587; 1994.

[23] Entman, M. L.; Youker, K.; Shoji, T.; Kukielka, G.; Shappell, S. B.; Taylor, A. A.; Smith, C. W. Neutrophil induced oxidative injury of cardiac myocytes. A compartment system requiring

CD11b/CD18-ICAM-1 adherence. *J. Clin. Invest.* **90:**1335–1345; 1992.

[24] Maresca, M.; Colao, C.; Leoncini, G. Generation of hydrogen peroxide in resting and activated platelets. *Cell. Biochem. Funct.* **10:**79–85; 1992.

[25] Wang, J. F.; Jerrells, T. R.; Spitzer, J. J. Decreased production of reactive oxygen intermediates is an early event during in vitro apoptosis of rat thymocytes. *Free Radic. Biol. Med.* **20:**533–542; 1996.

[26] Bass, D. A.; Parce, J. W.; Dechatelet, L. R.; Szejda, P.; Seeds, M. C.; Thomas, M. Flow cytometric studies of oxidative product formation by neutrophils: a graded response to membrane stimulation. *J. Immunol.* **130:**1910–1917; 1983.

[27] Carter, W. O.; Narayanan, P. K.; Robinson, J. P. Intracellular hydrogen peroxide and superoxide anion detection in endothelial cells. *J. Leukoc. Biol.* **55:**253–258; 1994.

[28] Suda, N.; Morita, I.; Kuroda, T.; Murota, S. Participation of oxidative stress in the process of osteoclast differentiation. *Biochim. Biophys. Acta* **1157:**318–323; 1993.

[29] Rabesandratana, H.; Fournier, A.-M.; Chateau, M.-T.; Serre, A.; Dornand, J. Increased oxidative metabolism in PMA-activated lymphocytes: a flow cytometric study. *Int. J. Immunopharmacol.* **14:**895–902; 1992.

[30] Shen, H.-M.; Shi, C.-Y.; Shen, Y.; Ong, C.-N. Detection of elevated reactive oxygen species level in cultured rat hepatocytes treated with aflatoxin B$_1$. *Free Radic. Biol. Med.* **21:**139–146; 1996.

[31] Takeuchi, T.; Nakajima, M.; Morimoto, K. Relationship between the intracellular reactive oxygen species and the induction of oxidative DNA damage in human neutrophil-like cells. *Carcinogenesis* **17:**1543–1548; 1996.

[32] Marchesi, E.; Rota, C.; Fann, Y. C.; Chignell, C. F.; Mason, R. P. Photoreduction of the fluorescent dye 2′-7′-dichlorofluorescin: a spin trapping and direct electron spin resonance study with implications for oxidative stress measurements. *Free Radic. Biol. Med.* **26:**148–161; 1999.

[33] Dunford, H. B.; Stillman, J. S. On the function and mechanism of action of peroxidases. *Coord. Chem. Rev.* **19:**187–251; 1976.

[34] Cathcart, R.; Schwiers, E.; Ames, B. N. Detection of picomole levels of hydroperoxides using a fluorescent dichlorofluorescein assay. *Anal. Biochem.* **134:**111–116; 1983.

[35] Hildebrandt, A. G.; Roots, I. Reduced nicotinamide adenine dinucleotide phosphate (NADPH)-dependent formation and breakdown of hydrogen peroxide during mixed function oxidation reactions in liver microsomes. *Arch. Biochem. Biophys.* **171:**385–397; 1975.

[36] Duling, D. R. Simulation of multiple isotropic spin-trap EPR spectra. *J. Magn. Reson. B.* **104:**105–110; 1994.

[37] Claiborne, A.; Fridovich, I. Chemical and enzymatic intermediates in the peroxidation of o-dianisidine by horseradish peroxidase. 2. Evidence for a substrate radical–enzyme complex and its reaction with nucleophiles. *Biochemistry* **18:**2329–2335; 1979.

[38] Krainev, A. G.; Williams, T. D.; Bigelow, D. J. Oxygen-centered spin adducts of 5,5-dimethyl-1-pyrroline *N*-oxide (DMPO) and 2*H*-imidazole 1-oxides. *J. Magn. Reson. B.* **111:**272–280; 1996.

[39] Buettner, G. R.; Mason, R. P. Spin-trapping methods for detecting superoxide and hydroxyl free radicals *in vitro* and *in vivo. Methods Enzymol.* **186:**127–133; 1990.

[40] Rothe, G.; Oser, A.; Valet, G. Dihydrorhodamine 123: a new flow cytometric indicator for respiratory burst activity in neutrophil granulocytes. *Naturwissenschaften* **75:**354–355; 1988.

[41] Crow, J. P. Dichlorodihydrofluorescein and dihydrorhodamine 123 are sensitive indicators of peroxynitrite *in vitro:* implications for intracellular measurement of reactive nitrogen and oxygen species. *Nitric Oxide* **1:**145–157; 1997.

[42] Kooy, N. W.; Royall, J. A.; Ischiropoulos, H.; Beckman, J. S. Peroxynitrite-mediated oxidation of dihydrorhodamine 123. *Free Radic. Biol. Med.* **16:**149–156; 1994.

[43] Back, S. A.; Gan, X.; Li, Y.; Rosenberg, P. A.; Volpe, J. J. Maturation-dependent vulnerability of oligodendrocytes to oxidative stress-induced death caused by glutathione depletion. *J. Neurosc.* **18:**6241–6253; 1998.

[44] Goossens, V.; Grooten, J.; De Vos, K.; Fiers, W. Direct evidence for tumor necrosis factor-induced mitochondrial reactive oxygen intermediates and their involvement in cytotoxicity. *Proc. Natl. Acad. Sci. USA* **92:**8115–8119; 1995.

[45] Larsen, L. N.; Dahl, E.; Bremer, J. Peroxidative oxidation of leuco-dichlorofluorescein by prostaglandin H synthase in prostaglandin biosynthesis from polyunsaturated fatty acids. *Biochim. Biophys. Acta* 1299:47–53; 1996.

ABBREVIATIONS

DCFH—2′-7′-dichlorofluorescin

DCFH-DA—2′-7′-dichlorofluorescin diacetate

DCF—2′-7′-dichlorofluorescein

DCF$^{\bullet -}$—DCF semiquinone free radical

DMPO—5,5-dimethyl-1-pyrroline *N*-oxide

DMSO—dimethyl sulfoxide

DTPA—diethylenetriamine pentaacetic acid

ESR—electron spin resonance

HRP—horseradish peroxidase

SOD—superoxide dismutase